Research Article | Vol. 30, No. 22 / 24 Oct 2022 / Optics Express 39922
Optics EXPRESS

Blister formation in dynamic release mirror structures using femtosecond laser pulses

ALAN T. K. GODFREY,[1] DEEPAK L. N. KALLEPALLI,[1,2] SABAA RASHID,[3] JESSE RATTÉ,[1] CHUNMEI ZHANG,[1] AND P. B. CORKUM[1,*]

[1]Joint Attosecond Science Laboratory, University of Ottawa and National Research Council of Canada, 100 Sussex Dr., Ottawa K1N 5A2, Canada
[2]Light Conversion USA, 201 South Wallace, Suite B-2C, Bozeman, MT 59715, USA
[3]Center for Research in Photonics, School of Electrical Engineering and Computer Science, University of Ottawa, Ottawa K1N 6N5, Canada
*pcorkum@uottawa.ca

Abstract: Blister formation occurs when a laser pulse interacts with the underside of a polymer film on a glass substrate and is fundamental in Laser-Induced Forward Transfer (LIFT). We present a novel method of controlling blister formation using a thin metal film situated between two thin polymer films. This enables a wide range of laser pulse energies by limiting the laser penetration in the film, which allows us to exploit nonlinear interactions without transmitting high intensities that may destroy a transfer material. We study blisters using a helium ion microscope, which images their interiors, and find that laser energy deposition is primarily in the metal layer and the top polymer layer remains intact. Blister expansion is driven by laser-induced spallation of the gold film. Our work shows that this technique could be a viable platform for contaminant-free LIFT using nonlinear absorption beyond the diffraction limit.

1. Introduction

Laser-Induced Forward Transfer (LIFT) has received a great deal of attention due to its versatility, simplicity, and its potential to deposit materials over length scales ranging from nanometers to millimeters [1–3]. LIFT involves focussing a laser pulse through a transparent support substrate onto the rear side of a thin film of the material to be transferred, which is called the donor. Another substrate, which is called the receiver, is placed on the donor material with or without a spacer to accept the transfer material [3–11].

There has been a transition from using a continuous-wave laser, as in the case of Laser-Induced Thermal Imaging (LITI), to nanosecond, picosecond, and femtosecond laser pulses in LIFT processes [12–14]. Advanced versions of LIFT use a dynamic release layer (DRL) between the donor and support substrate to minimise the contamination of the donor from direct interaction with the laser. The DRL absorbs laser light and provides thrust either by vaporizing fully, such as for a triazine film [2,3,14], or by partial heating or vaporization resulting in blister formation [4–6,10–12]. Ultrafast lasers with femtosecond pulse durations are preferred in achieving contaminant-free transfer as the energy deposition occurs with minimal thermal diffusion.

In addition to using femtosecond lasers, nonlinear absorption of light in materials plays an important role in small-scale material transfer at or below the diffraction limit (on the order of the wavelength of the laser). Work on polyimide blisters with 45-fs pulses using nonlinear absorption of 800 nm light showed sub-micrometer blister diameters (~700 nm full width at $1/e^2$) [15]. Similar work using 15-ns pulses at a wavelength of 355 nm in the linear absorption regime achieved blister sizes as small as ~10 μm, which was approximately the size of the laser spot [5]. Further, we demonstrated that the chemical changes induced by an ultrafast laser are confined below the polymer surface, leaving the surface chemically intact, as shown

#470141 https://doi.org/10.1364/OE.470141
Journal © 2022 Received 14 Jul 2022; revised 16 Sep 2022; accepted 19 Sep 2022; published 13 Oct 2022

Optics EXPRESS

through focussed ion beam and X-ray photoelectron spectroscopy techniques [16,17]. The size of laser-induced structures decreases with decreasing film thickness [18], but thinner films are more prone to rupture [5]. Therefore, minimizing the depth and width of laser energy deposition will enable thinner DRLs and thus smaller transfer sizes. Metal films have also been used as DRLs [10,11,19,20]. While these films have much smaller absorption depths, they can lead to contamination by fragments of metal in the transfer material [21].

We report a DRL called a dynamic release mirror structure (DRMS) that consists of a metal layer sandwiched between two polymer layers. It is capable of contaminant-free LIFT, since chemical changes are confined to the glass-polymer interface below the metal layer. It may also enhance the laser intensity and fluence inside of the film by forming a standing wave in the polymer below the metal layer that promotes formation of intact blisters below the threshold energy for a similar polymer film without a metal layer. The central metal layer may also absorb laser light and reflect excessive intensities which would otherwise be transmitted by a single nonlinearly absorbing polymer film and damage the donor. Additionally, the technique can be used from ultraviolet to near-infrared wavelengths and for all pulse durations since metals tend to be highly reflective and opaque over a broad range of wavelengths. The DRMS configuration combines the advantages of metals and polymers for DRL-based LIFT.

Figure 1 shows a schematic of our experimental setup. First, an ultrafast laser pulse at 800 nm wavelength is focussed onto the DRMS. At sufficiently high intensities, the borosilicate glass substrate may absorb 3 photons of 800 nm light based on its ~4 eV bandgap [22]. The remaining energy in the pulse reaches the DRMS. The first layer in the DRMS is a 400-nm-thick PMMA layer that may undergo nonlinear absorption to drive the expansion of a protruding blister. The energy left over is then reflected from the central metal layer, which may allow for the laser pulse to interfere with itself and enhance the intensity and fluence in regions of constructive interference. In cases where the initial pulse intensity and fluence is below the polymer absorption threshold, nonlinear absorption driven by standing-wave interference may dominate. PMMA has a similar bandgap to borosilicate glass [23,24]. In this case it will undergo three-photon absorption as well. Free-electron absorption may also happen directly in the gold layer [25]. The

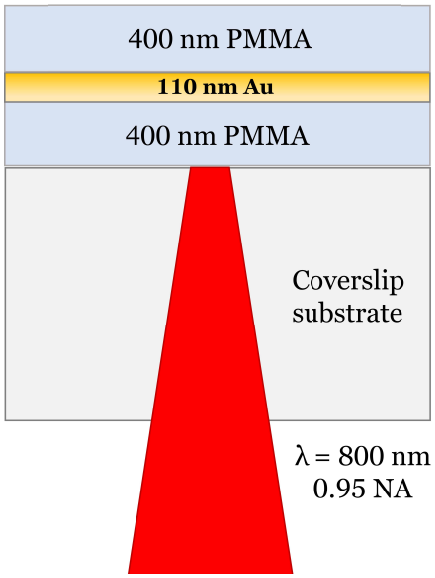

Fig. 1. A schematic showing a focussed laser pulse incident on the DRMS sample.

Optics EXPRESS

top layer is another 400-nm-thick PMMA layer which is not exposed to the laser. It acts as a "cap" on the DRMS to control the expansion and prevent film rupture that would contaminate a transfer material. In this paper, we form blisters in a DRMS and characterize the resulting blister heights and diameters. We then use a focussed gallium beam to dissect blisters and collect nanoscale images of their interiors using helium ion microscopy. Using this analysis, we assess the contributions of each layer to the blister formation process. Lastly, we comment on nonlinear absorption of the femtosecond pulses in the substrate before they reach the DRMS, and model the resulting fluences incident on the DRMS after propagation.

2. Experimental

We use the femtosecond-laser-induced blister formation experiment setup as shown in Ref. [15]. A Coherent RegA 9040 Ti:sapphire laser produces pulses with a central wavelength of 800 nm and durations of 45 fs (FWHM). Pulse durations were characterized using a MesaPhotonics MP002 FROGscan instrument. We pass the beam through a spatial filter and confirm that the beam has a Gaussian profile and a beam quality factor of $M^2 = 1.08 \pm 0.02$ using a DataRay WinCamD UCD12 beam profiler. We adjust the pulse energy using a variable attenuator consisting of a rotatable half-wave plate and a linear polarizer. We focus the laser using a 0.95-NA microscope objective (Leitz Wetzlar 80× 0.95-NA objective, stock no. 48728) mounted on a vertical motor stage to adjust the focal spot placement. The 10-mm entrance aperture of the objective was underfilled by a beam diameter of 4 mm, resulting in an estimated focal spot diameter of 2.6 µm. We measured the objective transmission to be 65.1% and estimate the net reflectivity of the sample to be 4.3% following the Fresnel coefficient analysis shown in Derrien *et al.* [26]. Pulse energies are given as measured before the microscope objective; losses are factored into all intensity and fluence values.

For sample fabrication, we use no. 1.5 Fisherbrand borosilicate glass coverslips (thicknesses of 0.16–0.19 mm) as substrates. Substrates are cleaned in acetone, isopropyl alcohol, and deionized water and dried on a hotplate. PMMA films are spin-coated with Microchem 495 PMMA A6 at a spin speed of 2000 revolutions/min for 30 s. This resulted in a film thickness of 400±50 nm for each layer of PMMA, measured using a Bruker Dektak XT contact profilometer. The gold layer in the DRMS was coated by thermal vapor deposition, and its thickness was determined to be 110±5 nm by using a JPK Nanowizard II BioAFM atomic force microscope in contact mode. We use the same method to characterize the surface morphology of laser-induced blisters after fabrication. We determined the net transmission of the DRMS to be 13% by passing the collimated laser beam through the sample.

We used a Zeiss ORION Nanofab helium ion microscope for characterizing the interior of blisters. The sample was mounted normal to the focussed gallium ion source, which was used to mill away half of each blister before imaging from a 54° angle using the helium ion beam. Prior to this, the sample was coated with 30 nm of aluminum to protect the film from damage from excessive gallium beam exposure.

3. Results and discussion

First, we fabricated blisters on the PMMA and DRMS samples in a back-illumination geometry as shown in Fig. 1. The laser pulse energy was adjusted from 40 nJ to 1.5 µJ. Fig. 2 shows the AFM scan profiles of height and diameter of the blisters for the DRMS sample.

We plot blister height and radius as a function of laser pulse energy in Fig. 3. The height of blisters should depend on how far the energy deposition penetrates the film and how much material remains to support the intact expansion of a blister. Under the given experimental conditions, we achieved blisters with heights of 350 nm at 200 nJ of pulse energy. Further increase in energy beyond 200 nJ caused blister rupture. Figure 3 indicates an increasing trend of

Optics EXPRESS

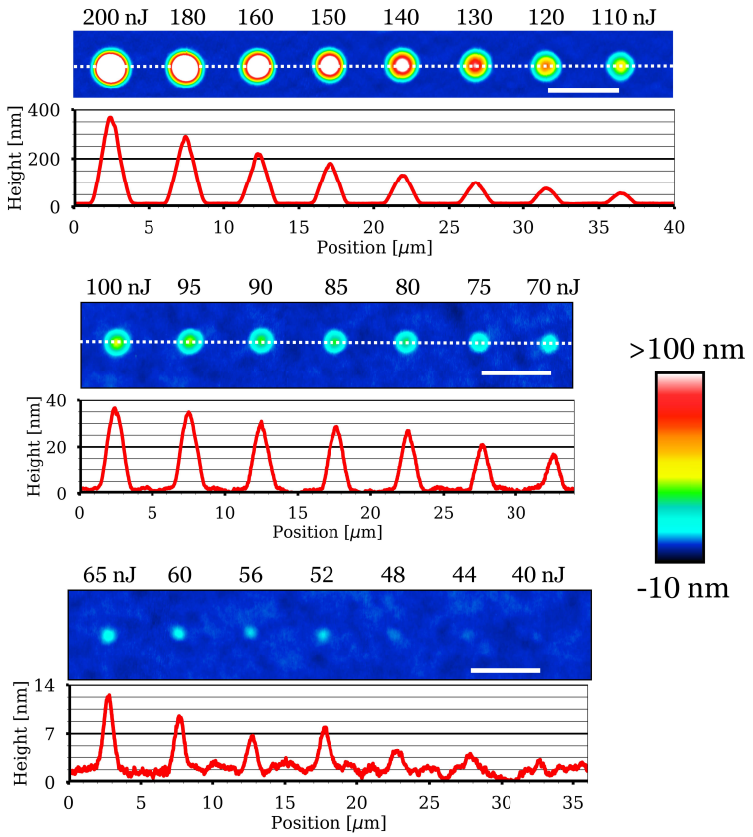

Fig. 2. AFM images and cross-sectional profiles of blisters created in the DRMS sample at different pulse energies. Scalebars are 5 μm in length.

height and diameter with pulse energy, and saturation of these values at energies near 200 nJ, before rupture occurs.

To understand the role of the gold layer in the DRMS, we then fabricated blisters on a sample with two 400-nm layers of PMMA only. Fig. 4 shows AFM scans of the laser-induced structures in the film. We did not observe any modification below 250 nJ of pulse energy. At 250 nJ, which is the energy threshold for modification (visual and morphological), we immediately saw film rupture which continued for all higher energies used. This comparison shows how an embedded metal layer in a polymer film greatly improves control of blister formation. With a thicker film of PMMA, intact blister formation may also occur, but this would result in larger structure sizes as discussed earlier, and does not address the issue of transmitted intensity below the nonlinear absorption threshold.

We examined blisters using the helium ion microscope. Fig. 5(a) shows a cross-sectional view blister made with a pulse energy of 300 nJ. This image was generated after one cut was made using the gallium milling beam. However, there was considerable material redeposition, evidenced by the lack of a sharp boundary between PMMA and the glass substrate. This was addressed by following with a second gallium beam cut using the same parameters but made over a smaller area to prevent redeposition. The image after the second gallium beam cut is shown in Fig. 5(b). The second cut greatly enhanced the contrast between each material but resulted in milling of small pockets from both PMMA layers. This was verified by performing similar

Optics EXPRESS

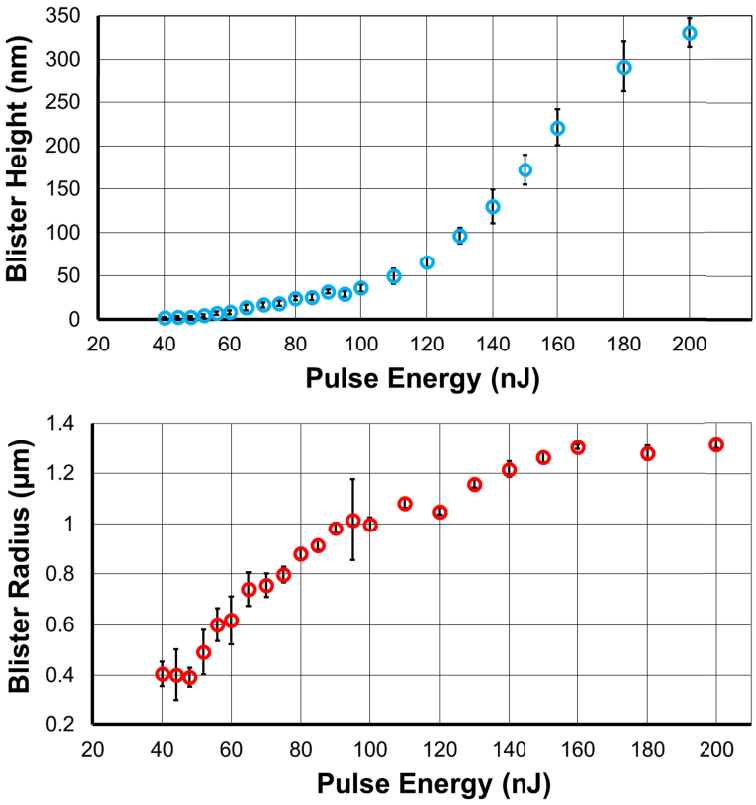

Fig. 3. Trends in blister height (above) and blister diameter (below) with pulse energy. Near the threshold pulse energy of 40 nJ, blister heights are on the scale of the surface roughness. Beyond 200 nJ of pulse energy, blisters were not left intact and showed rupture.

gallium beam cuts on a pristine region of the sample. These pockets should not be confused with the initial laser modification.

In Fig. 5(a) and 5(b), we see the gold layer has been disrupted, and resolidified gold has collected in the top layer of PMMA. The PMMA close to the melted gold has also been modified, as seen by its contrast. In the center of the structure, there is a small ablated region in the bottom PMMA layer. The ablated region could be due to increased fluence due to standing-wave interference caused by reflection from the gold layer. We expect the highest fluence enhancement from this effect at the first constructive interference antinode ~ 130 nm (λ/4 in the medium) away from the gold film. Gold is highly reflective, but ultrafast changes to gold reflectivity should be considered. In the work by Apalkov and Stockman, the reflectivity of metal nanofilms was reduced by a factor of ~ 3 at an electric field strength of 3 V/Å [27]. In our work, the breakdown intensity of borosilicate glass limits the field strength to ~ 0.8 V/Å, and the film thickness is several times the skin depth, so total reflectivity should not be greatly affected. Lastly, a small crack in the top PMMA layer is visible, where the aluminum coating has entered. We have observed similar cracks in polyimide blisters with excessive pulse energies [15]. Still higher pulse energies lead to rupture of the structures.

Figure 5(c) and 5(d) show the same measurements performed for a blister made with 180 nJ of pulse energy. Similar features are seen, but at this energy we see laser-modified gold layer forms an intact ball of gold that stays partially connected to the underlying film. Similar observations of ultrafast laser spallation of ultrathin gold films on glass have been reported for front illumination,

Optics EXPRESS

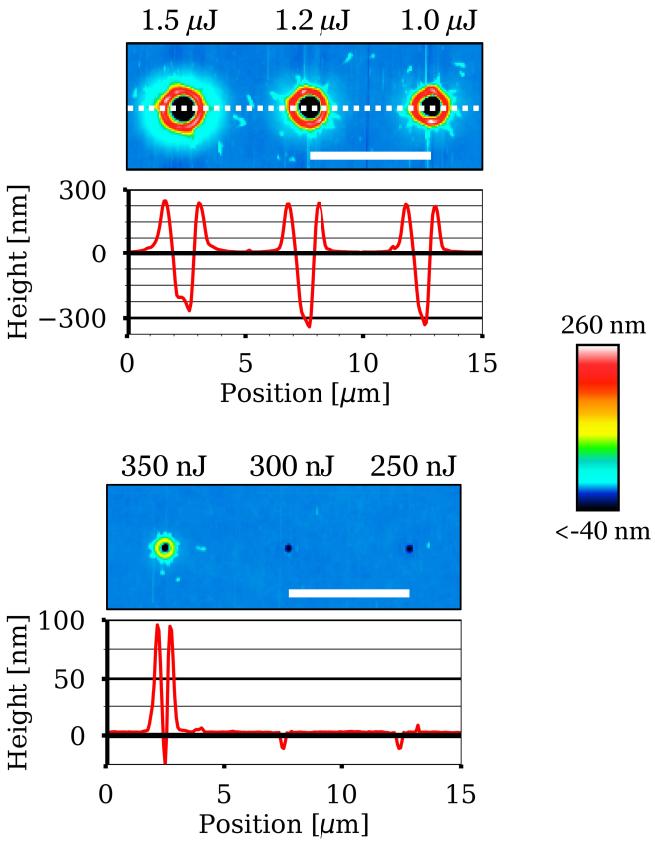

Fig. 4. AFM images of ablation spots on the PMMA sample at different pulse energies. No intact blister formation was seen. Scalebars are 5 μm in length.

where pulses of moderate energy allow the melted gold to cool and become trapped due to surface tension [28]. It should be noted that the characteristic two-temperature heating length of gold was 120 nm, which is approximately the thickness of our gold film; hence the results for front and back incidence are analogous. Similar droplet formation has also been observed in laser-based printing of silicon nanoparticles using femtosecond pulses [29].

We now consider the intensities and fluences leading to the blister formation and PMMA ablation in this experiment. Intensity is the key quantity for multiphoton ionization, whereas fluence is the key quantity for ablation and similar processes [14,25,30,31]. The spherical aberration of our objective causes axial stretching of the focus resulting in reduced intensity in the focus [32]. Also, as established by Rayner *et al.* [33], an intense pulse focussed through glass can be attenuated by ionization of the medium, which limits the peak intensity of the pulse. In our case, intensities above 13 TW/cm^2 will break down borosilicate glass and be lost to the medium before reaching the film [34]. The peak intensity is strictly limited, but the peak fluence of a Gaussian pulse (determined by integrating over the temporal extent of the pulse) may still increase.

Figure 6 shows modelled values for peak fluences at the DRMS under experimental conditions, accounting for nonlinear absorption in the borosilicate glass substrate before reaching the DRMS. We estimate that, with an aberration-based axial stretch of the focus by a factor of 2.0 to 3.1 (which decreases the laser intensity and fluence), the resulting fluence thresholds for blister formation range from 0.30–0.47 J/cm^2 at an input pulse energy of 40 nJ. This estimate was

Optics EXPRESS

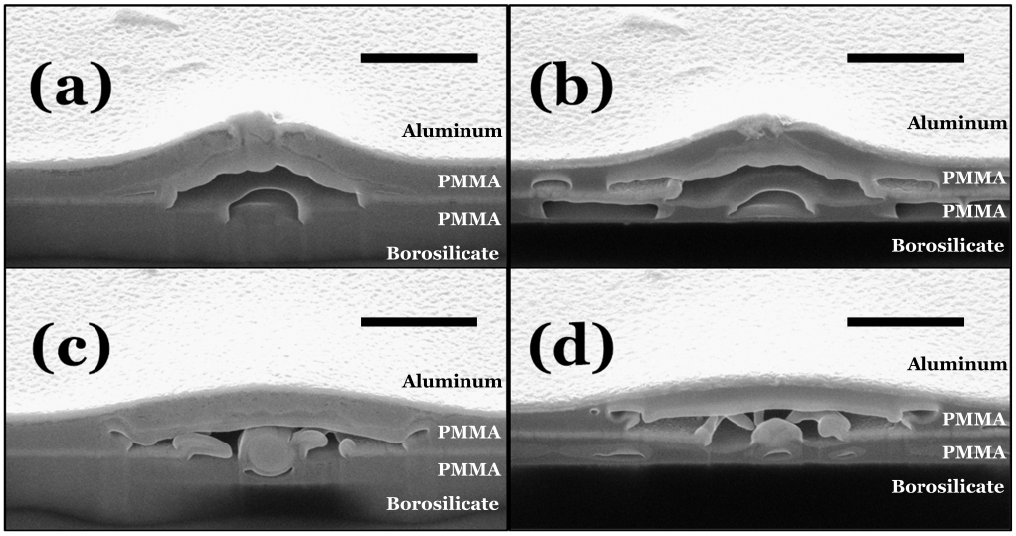

Fig. 5. Helium ion microscope images of blisters in the DRMS sample that have been sectioned by a gallium beam. Scalebars are 1 μm in length. A blister made using 300 nJ of pulse energy is shown (a) after one cut from the gallium beam and (b) after a second cut to remove redeposited material which obscures material boundaries in the image. The process was repeated in (c) and (d) for a blister made using 180 nJ of pulse energy. The central gold layer, unmodified and modified PMMA, borosilicate glass substrate and aluminum protective layer are all resolvable by contrast.

made by scaling the peak intensity and fluence by a constant factor to match known threshold values for femtosecond laser ablation of ultrathin gold films. For a film of approximately 100 nm thickness, the fluence threshold for ablation is approximately 0.3–0.5 J/cm^2 [25]. Absorption in the glass did not occur at the DRMS blister formation threshold (40 nJ of pulse energy), since the peak intensity was too low to ionize borosilicate glass (<10 TW/cm^2 at maximum). However, nonlinear absorption in the glass substrate began to occur at 55–80 nJ of pulse energy according to our model.

In the case of the PMMA-only film, the onset of damage occurred at approximately 1.0–1.1 J/cm^2, which is approximately one-third of the fluence that would be reached in absence of the nonlinearly-absorbing glass substrate. Even without the aberration (axial stretch factor of 1), the peak fluence would only reach 1.3 J/cm^2. Given a refractive index of 1.49 at 800 nm [35], the normal incidence reflectance of the PMMA-air interface is 0.039, which would lead to a standing-wave intensity and fluence increase of 43% [36]. Even then, our fluences are lower than the literature values for ablation of bulk PMMA with similar laser parameters, 2.3–2.9 J/cm^2 [31,37]. The high NA and spherical aberration may result in light rays that are no longer normal to the PMMA-air interface everywhere in the focus. Deviation from normal incidence would increase the reflectivity and hence may further enhance the local intensity and fluence due to a standing wave.

Our results indicate that the driving mechanism of blister expansion is laser spallation of the gold film. However, the top polymer layer confined the molten gold, which would allow contaminant-free LIFT using this scheme. Additionally, the thickness of the polymer layer provides a way to selectively dampen the expansion process independent of the metal layer. The bottom layer of polymer played a small role in the experiment, but nonlinear absorption in this layer could be driven more easily with selection of a substrate such as fused silica, which has a

Optics EXPRESS

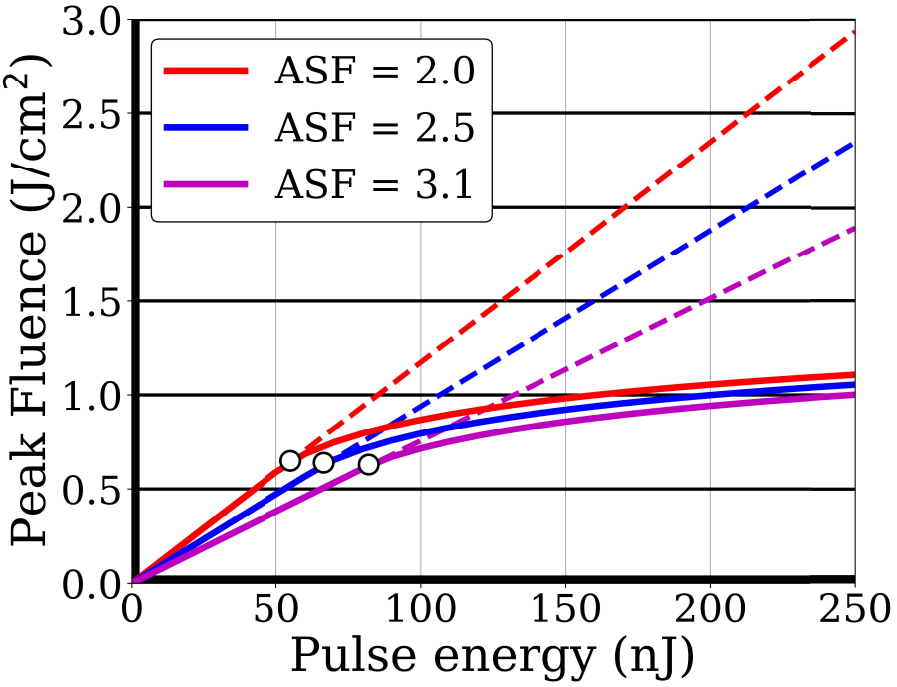

Fig. 6. Modelled peak fluence of laser pulses after passing through the borosilicate glass substrate. ASF = axial stretch factor. Pulse energy is given before transmission losses and nonlinear absorption by the glass. The dashed lines indicate the peak fluence in vacuum conditions. The white breakpoints on each line indicate when the intensity reaches the breakdown threshold for borosilicate glass.

much higher bandgap (~ 9 eV) [22]. This would allow for higher intensities in the substrate and less loss from nonlinear absorption in glass for a given pulse energy, increasing the maximum fluence at the DRMS. Alternatively, the fluence at the DRMS could be increased by lengthening the femtosecond pulse, reducing the intensity (and hence substrate losses) for a given pulse energy, or by reducing the bandgap of the polymer by material selection.

4. Conclusion

We have developed a multilayer configuration for blister formation that offers comparable spatial resolution to our previous work [15] with the added advantages of reduced intensity at the donor material and more parameters for optimization of the blister formation process. We studied the high-intensity interaction with the multilayer film and substrate and determined that the interaction with the gold layer drives blister formation through free-electron absorption leading to ablation. Nonlinear absorption in the polymer also occurs, but was suppressed due to nonlinear absorption in the glass substrate before reaching the DRMS. As a result, the magnitude of this effect was much smaller than blister expansion due to gold ablation. Future steps such as choosing optimal substrate and pulse materials, as well as pulse broadening, could enhance the role of the bottom PMMA later in the process. However, a two-layer polymer-on-metal approach could also be adopted. When the metal film gives rise to laser-induced blister formation, the ultimate spatial resolution limit should depend on the heat diffusion length in the metal layer. This could be improved by choosing a metal with lower thermal conductivity such as chromium, nickel, steel or

Optics EXPRESS

titanium. The top layer of PMMA stayed intact during blister formation in the DRMS, which would act as a barrier to thermal damage and contamination in a LIFT process.

The multilayer approach to blister formation provides access to nonlinear processes in thin films of metal and polymer without risking damage or contamination to a transfer material in LIFT. It combines the advantages of polymers and metals as dynamic release layers while also mitigating the drawbacks of using each material separately. It can be used for improving resolution of blister-based LIFT, but it could also be used in existing microscale applications for enhanced control and flexibility. While our work has focussed on using nonlinear processes on scales near the diffraction limit, the DRMS approach may also be interesting to apply with use with linear absorption of nanosecond pulses for greater tunability of the LIFT process.

Funding. Natural Sciences and Engineering Research Council of Canada (EGP 213 523138-18, RGPIN-2019-04603); Ontario Centres of Excellence (29119); Standard BioTools Inc.; Canada Foundation for Innovation.

Acknowledgments. We acknowledge funding from Natural Sciences and Engineering Research Council of Canada (NSERC) Engage (Grant No. EGP 523138-18) and Discovery (Grant No. RGPIN-2019- 04603) grants, the Ontario Centres of Excellence Voucher for Innovation and Productivity I Program (Grant No. 29119), Standard BioTools Inc., and the Canada Foundation for Innovation. A.T.K.G. acknowledges financial support from the NSERC's Postgraduate Scholarship – Doctoral and the University of Ottawa's Excellence Scholarship. S.R. thanks Pierre Berini for the insightful discussions.

Disclosures. The authors declare no conflicts of interest.

Data availability. Data underlying the results presented in this paper are not publicly available at this time but may be obtained from the authors upon reasonable request.

References

1. J. Bohandy, B. F. Kim, and F. J. Adrian, "Metal deposition from a supported metal film using an excimer laser," J. Appl. Phys. **60**(4), 1538–1539 (1986).
2. D. P. Banks, C. Grivas, J. D. Mills, R. W. Eason, and I. Zergioti, "Nanodroplets deposited in microarrays by femtosecond Ti:sapphire laser-induced forward transfer," Appl. Phys. Lett. **89**(19), 193107 (2006).
3. D. P. Banks, K. Kaur, R. Gazia, R. Fardel, M. Nagel, T. Lippert, and R. W. Eason, "Triazene photopolymer dynamic release layer-assisted femtosecond laser-induced forward transfer with an active carrier substrate," Europhys. Lett. **83**(3), 38003 (2008).
4. N. T. Kattamis, P. E. Purnick, R. Weiss, and C. B. Arnold, "Thick film laser induced forward transfer for deposition of thermally and mechanically sensitive materials," Appl. Phys. Lett. **91**(17), 171120 (2007).
5. M. S. Brown, N. T. Kattamis, and C. B. Arnold, "Time-resolved study of polyimide absorption layers for blister-actuated laser-induced forward transfer," J. Appl. Phys. **107**(8), 083103 (2010).
6. M. S. Brown, C. F. Brasz, Y. Ventikos, and C. B. Arnold, "Impulsively actuated jets from thin liquid films for high-resolution printing applications," J. Fluid Mech. **709**, 341–370 (2012).
7. N. T. Kattamis, M. S. Brown, and C. B. Arnold, "Finite element analysis of blister formation in laser-induced forward transfer," J. Mater. Res. **26**(18), 2438–2449 (2011).
8. J. P. McDonald, V. R. Mistry, K. E. Ray, S. M. Yalisove, J. A. Nees, and N. R. Moody, "Femtosecond-laser-induced delamination and blister formation in thermal oxide films on silicon (100)," Appl. Phys. Lett. **88**(15), 153121 (2006).
9. J. R. Serrano and D. G. Cahill, "Laser-Induced Blistering of Thin SiO2 on Si," Microscale Thermophys. Eng. **9**(2), 155–164 (2005).
10. N. T. Goodfriend, S. V. Starinskiy, O. A. Nerushev, N. M. Bulgakova, A. V. Bulgakov, and E. E. B. Campbell, "Laser pulse duration dependence of blister formation on back-radiated Ti thin films for BB-LIFT," Appl. Phys. A **122**(3), 154 (2016).
11. N. T. Goodfriend, S. Y. Heng, O. A. Nerushev, A. V. Gromov, A. V. Bulgakov, M. Okada, W. Xu, R. Kitaura, J. Warner, H. Shinohara, and E. E. B. Campbell, "Blister-based-laser-induced-forward-transfer: a non-contact, dry laser-based transfer method for nanomaterials," Nanotechnology **29**(38), 385301 (2018).
12. L. Rapp, A. P. Alloncle, A. K. Diallo, S. Nénon, C. Videlot-Ackermann, F. Fages, and P. Delaporte, "Pulsed-Laser Printing Process for Organic Thin Film Transistors Fabrication," AIP Conf. Proc. **1278**, 824–831 (2010).
13. M. B. Wolk, J. P. Baetzold, E. Bellmann, T. R. H. Jr., S. Lamansky, Y. Li, R. R. Roberts, V. Savvateev, J. S. Staral, and W. A. Tolbert, "Laser thermal patterning of OLED materials," in *Organic Light-Emitting Materials and Devices VIII*, vol. 5519 Z. H. Kafafi and P. A. Lane, eds., International Society for Optics and Photonics (SPIE, 2004).
14. K. S. Kaur, R. Fardel, T. C. May-Smith, M. Nagel, D. P. Banks, C. Grivas, T. Lippert, and R. W. Eason, "Shadowgraphic studies of triazene assisted laser-induced forward transfer of ceramic thin films," J. Appl. Phys. **105**(11), 113119 (2009).
15. A. T. Godfrey, D. L. Kallepalli, J. Ratté, C. Zhang, and P. Corkum, "Femtosecond-Laser-Induced Nanoscale Blisters in Polyimide Thin Films through Nonlinear Absorption," Phys. Rev. Appl. **14**(4), 044057 (2020).

Optics EXPRESS

16. D. L. N. Kallepalli, A. T. K. Godfrey, J. Walia, F. Variola, A. Staudte, C. Zhang, Z. J. Jakubek, and P. B. Corkum, "Multiphoton laser-induced confined chemical changes in polymer films," Opt. Express **28**(8), 11267–11279 (2020).
17. D. L. N. Kallepalli, A. T. K. Godfrey, J. Ratté, A. Staudte, C. Zhang, and P. B. Corkum, "Surface adhesion of back-illuminated ultrafast laser-treated polymers," Phys. Rev. Mater. **5**(4), 045201 (2021).
18. V. Sametoglu, V. T. K. Sauer, and Y. Y. Tsui, "Production of 70-nm Cr dots by laser-induced forward transfer," Opt. Express **21**(15), 18525–18531 (2013).
19. J. M. Fitz-Gerald, A. Piqué, D. B. Chrisey, P. D. Rack, M. Zeleznik, R. C. Y. Auyeung, and S. Lakeou, "Laser direct writing of phosphor screens for high-definition displays," Appl. Phys. Lett. **76**(11), 1386–1388 (2000).
20. B. Hopp, T. Smausz, Z. Antal, N. Kresz, Z. Bor, and D. Chrisey, "Absorbing film assisted laser induced forward transfer of fungi (Trichoderma conidia)," J. Appl. Phys. **96**(6), 3478–3481 (2004).
21. N. T. Kattamis, N. D. McDaniel, S. Bernhard, and C. B. Arnold, "Laser direct write printing of sensitive and robust light emitting organic molecules," Appl. Phys. Lett. **94**(10), 103306 (2009).
22. M. Lenzner, J. Krüger, S. Sartania, Z. Cheng, C. Spielmann, G. Mourou, W. Kautek, and F. Krausz, "Femtosecond Optical Breakdown in Dielectrics," Phys. Rev. Lett. **80**(18), 4076–4079 (1998).
23. S. B. Aziz, O. G. Abdullah, A. M. Hussein, and H. M. Ahmed, "From Insulating PMMA Polymer to Conjugated Double Bond Behavior: Green Chemistry as a Novel Approach to Fabricate Small Band Gap Polymers," Polymers **9**(11), 626 (2017).
24. Q. M. Al-Bataineh, A. A. Ahmad, A. M. Alsaad, and A. D. Telfah, "Optical characterizations of PMMA/metal oxide nanoparticles thin films: bandgap engineering using a novel derived model," Heliyon **7**(1), e05952 (2021).
25. J. Krüger, D. Dufft, R. Koter, and A. Hertwig, "Femtosecond laser-induced damage of gold films," Appl. Surf. Sci. **253**(19), 7815–7819 (2007).
26. T. J.-Y. Derrien, R. Koter, J. Krüger, S. Höhm, A. Rosenfeld, and J. Bonse, "Plasmonic formation mechanism of periodic 100-nm-structures upon femtosecond laser irradiation of silicon in water," J. Appl. Phys. **116**(7), 074902 (2014).
27. V. Apalkov and M. I. Stockman, "Metal nanofilm in strong ultrafast optical fields," Phys. Rev. B **88**(24), 245438 (2013).
28. N. Inogamov, V. Zhakhovsky, and K. Migdal, "Laser-induced spalling of thin metal film from silica substrate followed by inflation of microbump," Appl. Phys. A **122**(4), 432 (2016).
29. U. Zywietz, T. Fischer, A. Evlyukhin, C. Reinhardt, and B. Chichkov, "Laser Printing of Nanoparticles," in *Laser Printing of Functional Materials* (John Wiley & Sons, Ltd., 2018), pp. 251–268.
30. D. P. Banks, K. Kaur, and R. W. Eason, "Influence of optical standing waves on the femtosecond laser-induced forward transfer of transparent thin films," Appl. Opt. **48**(11), 2058 (2009).
31. J.-M. Guay, A. Villafranca, F. Baset, K. Popov, L. Ramunno, and V. R. Bhardwaj, "Polarization-dependent femtosecond laser ablation of poly-methyl methacrylate," New J. Phys. **14**(8), 085010 (2012).
32. L. Capuano, R. Pohl, R. M. Tiggelaar, J. W. Berenschot, J. G. E. Gardeniers, and G. R. B. E. Römer, "Morphology of single picosecond pulse subsurface laser-induced modifications of sapphire and subsequent selective etching," Opt. Express **26**(22), 29283–29295 (2018).
33. D. M. Rayner, A. Naumov, and P. B. Corkum, "Ultrashort pulse non-linear optical absorption in transparent media," Opt. Express **13**(9), 3208–3217 (2005).
34. A. Ben-Yakar and R. L. Byer, "Femtosecond laser ablation properties of borosilicate glass," J. Appl. Phys. **96**(9), 5316–5323 (2004).
35. N. Sultanova, S. Kasarova, and I. Nikolov, "Dispersion Properties of Optical Polymers," Acta Phys. Pol. A **116**(4), 585–587 (2009).
36. This is calculated by the standard equation for intensity/fluence of an interfering wave. In terms of intensity, $I_{total} = I_1 + I_2 + 2\sqrt{I_1 I_2}\sin\phi$ where I_1 is the incident intensity, I_2 is the intensity of the reflected light, and ϕ is the phase difference between the incident and reflected light at some location in space. The enhancement factor is found by setting $I_2 = RI_1$ where R is the reflectance of the PMMA, and taking $\sin\phi = 1$ for fully constructive interference at an antinode.
37. S. Baudach, J. Bonse, J. Krüger, and W. Kautek, "Ultrashort pulse laser ablation of polycarbonate and polymethylmethacrylate," Appl. Surf. Sci. **154-155**, 555–560 (2000).